ELSEVIER

Chemistry & Biology 8 (2001) 123–131

Chemistry & Biology

www.elsevier.com/locate/chembiol

Research Paper

New fluorescent probes for the measurement of cell membrane viscosity

Mark A. Haidekker [a], Taotao Ling [b], Michael Anglo [b], Hazel Y. Stevens [a], John A. Frangos [a], Emmanuel A. Theodorakis [b,*]

[a] *Department of Bioengineering, University of California, San Diego, 9500 Gilman Drive, La Jolla, CA 92093-0412, USA*
[b] *Department of Chemistry and Biochemistry, University of California, San Diego, 9500 Gilman Drive, MC 0358, La Jolla, CA 92093-0358, USA*

Received 10 October 2000; revisions requested: 7 November 2000 revisions received 24 November 2000; accepted 27 November 2000
First published online 19 December 2000

Abstract

Background: Molecular rotors are fluorescent molecules that exhibit viscosity-dependent fluorescence quantum yield, potentially allowing direct measurements of cell membrane viscosity in cultured cells. Commercially available rotors, however, stain not only the cell membrane, but also bind to tubulin and migrate into the cytoplasm. We synthesized molecules related to 9-(dicyanovinyl)-julolidine (DCVJ), which featured hydrocarbon chains of different length to increase membrane compatibility.

Results: Longer hydrocarbon chains attached to the fluorescent rotor reduce the migration of the dye into the cytoplasm and internal compartments of the cell. The amplitude of the fluorescence response to fluid shear stress, known to decrease membrane viscosity, is significantly higher than the response obtained from DCVJ. Notably a farnesyl chain showed a more than 20-fold amplitude over DCVJ and allowed detection of membrane viscosity changes at markedly lower shear stresses.

Conclusions: The modification of molecular rotors towards increased cell membrane association provides a new research tool for membrane viscosity measurements. The use of these rotors complements established methods such as fluorescence recovery after photobleaching with its limited spatial and temporal resolution and fluorescence anisotropy, which has low sensitivity and may be subject to other effects such as deformation.

Keywords: Cell membrane; Fluid shear stress; Fluorescence; Molecular rotor

1. Introduction

Membrane viscosity is a physical property of the cell, which describes the movement of molecules within the phospholipid bilayer. In general, membrane viscosity depends on the chemical composition of the bilayer and is shown to have optimum values for the proper function of various membrane-bound enzymes and receptors. For example, artificial phospholipid bilayers were found to have viscosity values between 70 and 120 cP, depending on the temperature [1], while in human epidermal cells, viscosity values ranging from 30 to 100 cP have been reported [2]. In liver cells, viscosities ranged from 108 to 217 cP [3].

Depending on the membrane viscosity (or membrane fluidity, which is its reciprocal), phospholipids and membrane-bound proteins show different vertical and lateral displacements, as well as lateral and rotational diffusion behavior [4]. Consequently, changes in membrane viscosity have been linked with alterations in physiological properties, such as carrier-mediated transport, activities of membrane-bound enzymes and receptor binding [5]. In addition, variations in membrane viscosity are linked to a variety of diseases, such as atherosclerosis [6], cell malignancy [7], hypercholesterolemia [8] and diabetes [9,10]. Further examples include an increase in membrane viscosity in several blood cells and specific brain cells in patients with Alzheimer's disease [11,12]. Increased membrane viscosity is also associated with aging [13]. Erythrocytes showed permanently increased membrane viscosity, thus altering hepatic microcirculation [14]. Furthermore, endothelial cells are able to sense fluid shear stress through the cell membrane [15] and effect changes that serve to maintain a specific level of flow in blood vessels [16].

* Correspondence: Emmanuel A. Theodorakis; E-mail: etheodor@ucsd.edu

1074-5521/01/$ – see front matter
PII: S1074-5521(00)00061-2

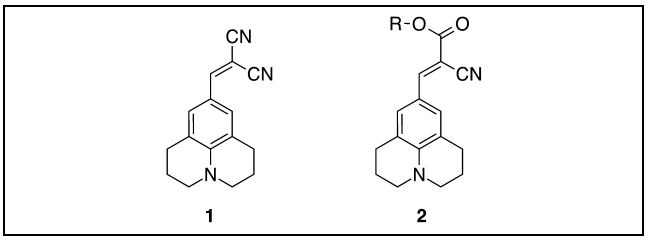

Fig. 1. Chemical structure of DCVJ (**1**) and the basic structure of the compounds synthesized. One of the nitrile functionalities of DCVJ has been replaced by a carboxylic group, allowing the addition of hydrocarbon chains R.

The importance of membrane viscosity in cellular biology and physiology led to the development of fluorescent-based methods for quantitative measurements. To date, there are three dominant methods to measure membrane viscosity: (a) fluorescence recovery after photobleaching (FRAP), in which measurement of the diffusivity of a fluorophore in the membrane is related to membrane viscosity [17], (b) fluorescence anisotropy, in which the out-of-plane rotation of a fluorophore is related to membrane viscosity [18] and (c) use of environment-sensitive fluorescent probes. In the latter category are included compounds such as 2-dimethylamino-6-lauroylnaphthalene, whose emission wavelength shifts with the viscosity of the medium [19] and 9-(dicyanovinyl)-julolidine (DCVJ, **1**) with a viscosity-dependent fluorescence quantum yield.

The intriguing fluorescent properties of DCVJ (Fig. 1) rest upon its ability to lose excited state energy either by radiation or by intramolecular rotation, the ratio of which depends on the free volume of the microenvironment [20]. This ability has defined a new class of molecules, commonly referred to as molecular rotors, that were found to react instantly (within 10 ns) to changes in the environment, thereby allowing real-time measurements with high temporal and spatial resolution. Moreover, in the case of DCVJ, its fluorescence quantum yield was shown to increase by a factor of 30 when the solvent was changed from 1-propanol to glycerol [1]. Due to the above properties, DCVJ has been employed to address a wide variety of problems, including polymerization processes [20], tubulin remodeling [21], and membrane viscosity measurements in liposomes and micelles [1]. More recently, DCVJ was employed to probe changes of membrane viscosity induced by fluid shear stress in cultured cells [22]. Nonetheless, the use of DCVJ in membrane viscosity measurements is often limited by its poor water solubility, which renders the preparation of DCVJ-based staining solutions problematic. For experiments on liposomes [1], this difficulty can be overcome by preparing a DCVJ-stained phospholipid base before forming the liposomes. In cultured cells, DCVJ can be bound to serum proteins [22], but their binding capacity is limited. Furthermore, protein-bound DCVJ migrates readily into the cytoplasm, thus adding a high level of constant background signal during biophysical measurements thereby reducing the sensitivity of the probe.

In light of the side effects mentioned above, it was deemed desirable to obtain a fluorescent molecule that has the viscosity-dependent properties of DCVJ, but shows a higher affinity to the cell membrane. For this purpose, we synthesized various compounds (**2a**–**2g**), in which one of the nitrile functions of DCVJ was replaced by a carboxylic ester bearing aliphatic hydrocarbon chains of different length. Our results demonstrate clearly that it is possible to alter the chemical structure of DCVJ, as shown in Fig. 1, without affecting its viscosity-dependent fluorescence properties. Specifically, compounds **2b**–**2g** have very similar viscosity-dependent fluorescence properties with DCVJ, but improved membrane localization. Moreover, the farnesyl-containing probe **2g** (farnesyl-(2-carboxy-2-cyanovinyl)-julolidine, FCVJ) displayed a dramatically (more than 20-fold) higher sensitivity than DCVJ when probing membrane viscosity changes and was shown to be more stable than **1** against photobleaching.

2. Results

2.1. Synthesis of the molecular rotors

The synthesis of compounds **2a**–**2g** is shown in Fig. 2. Commercially available (Aldrich) julolidine **3** was formylated with phosphorus oxychloride and dimethylformamide to afford aldehyde **4** in a 95% yield. The desired β-cyanoesters **7** were obtained via dicyclohexyl carbodii-

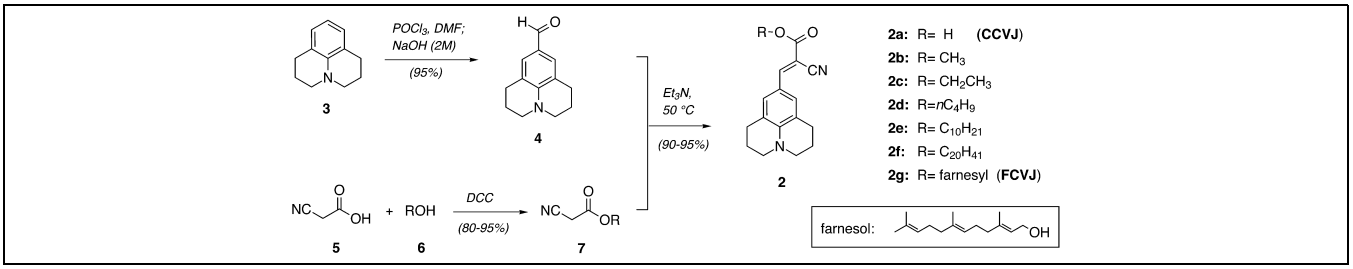

Fig. 2. Synthesis of the compounds **2a**–**2g**. Julolidine **3** was formylated to afford julolidine aldehyde **4**. The β-cyanosters **7** were obtained by esterification of cyanoacetic acid **5** with the corresponding alcohol **6**. Condensation of the esters **7** with julolidine aldehyde **4** produced the desired probes **2**.

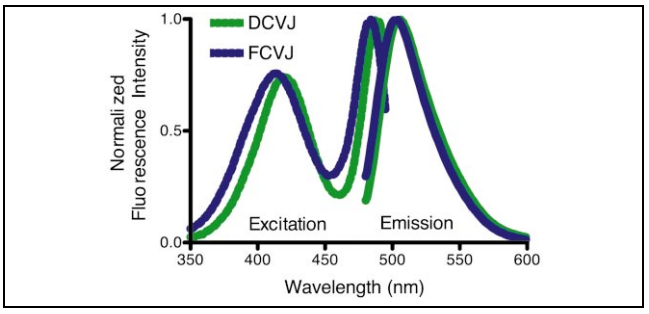

Fig. 3. Excitation spectra (dashed lines) and emission spectra (solid lines) for DCVJ and FCVJ in ethylene glycol. The spectra of the other compounds are similar. All probes exhibit a double excitation maximum in the blue range, and a single emission maximum in the green range.

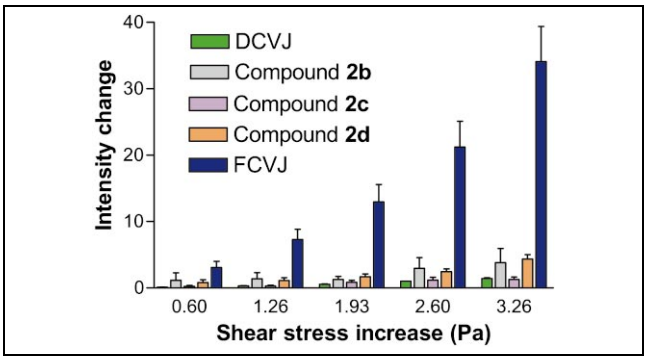

Fig. 4. Changes of fluorescence intensity as a function of the increase of shear stress for compounds **2b**, **2c**, **2d** and **2g** (FCVJ), as well as for DCVJ. All compounds except **2c** differ significantly ($P < 0.0001$) from DCVJ.

mide-induced esterification of cyanoacetic acid (**5**) with the corresponding alcohols in 80–95% yield. Condensation of esters **7** with aldehyde **4** in the presence of triethylamine produced the desired probes **2a**–**2g** in very good yields (90–95%). These compounds were purified by chromatography on silica gel and crystallized twice prior to use.

2.2. *Physical properties of the synthesized probes*

Absorption and emission maxima of the examined compounds were all in the blue and green range, respectively, with emission maxima between 490 and 505 nm and two distinctly different excitation maxima. The first lies at about 405 nm, and the second, major, maximum in the range of 450–490 nm. Fig. 3 shows the excitation and emission spectra of DCVJ and FCVJ. The other compounds exhibited very similar spectra. The excitation and emission maxima are listed for all compounds in Table 1.

All compounds exhibited a viscosity-dependent fluorescence emission, while a viscosity-dependent change of the emission wavelength could not be detected. Using media with different viscosities (different mixtures of glycerol and ethylene glycol), it was possible to verify the double logarithmic relationship of quantum yield and viscosity (Förster–Hoffmann equation, Eq. 3) which was established for DCVJ [1,15]. Furthermore, all compounds showed similar values of x in Eq. 3. This indicates that the photophysical properties of the molecular rotor had not been affected by the attachment of the hydrocarbon chain.

Only **2a** is water-soluble. Therefore, staining solutions were prepared using fetal calf serum (FCS) and bovine serum albumin (BSA) as carriers. All compounds, with the exception of **2f**, could be solubilized in aqueous media by binding it to BSA. Using FCS as a carrier, compounds **2e** and **2f** were insoluble, and compound **2d** as well as DCVJ showed a low solubility with precipitates forming within a few hours after the media preparation. The cells grown and stained on the flow chamber glass slides also exhibited the characteristic fluorescence emission spectrum of DCVJ. Under the microscope, the staining of the cells could be observed. In spite of its direct water solubility, **2a** was the only probe that did not stain the cell membrane in a significant way.

Table 1
Summary of the properties of each compound

Compound	Absorption and emission maxima (nm)[a]	$\phi = f(\eta)$ (slope x)[b]	Stains cell membrane	Response to shear stress[c]
(**1**) DCVJ	489/505	0.58	yes	0.38
(**2a**) R = H	454/489	(*)	no	n.a.
(**2b**) R = CH_3	485/504	0.67	yes	1.09
(**2c**) R = C_2H_5	486/503	0.6	yes	0.41
(**2d**) R = nC_4H_9	473/500	0.6	yes	1.11
(**2e**) R = $nC_{10}H_{21}$	458/499	(*)	yes	(*)
(**2f**) R = $nC_{20}H_{41}$	477/491	0.49	n.a.[d]	n.a.
(**2g**) R = farnesyl	483/503	0.56	yes	8.78

$\phi = f(\eta)$ refers to the dependency of the quantum yield ϕ on the viscosity η of the medium. (*) Not measured.
[a] Compounds dissolved in ethylene glycol.
[b] In Eq. 3, x represents the slope of a line fitted into the data points $\log \phi$ over $\log \eta$.
[c] Slope of regression line into the data points of Fig. 4 under the assumption of a linear relationship.
[d] Compound **2f** is insoluble in DMSO, methanol and ethanol.

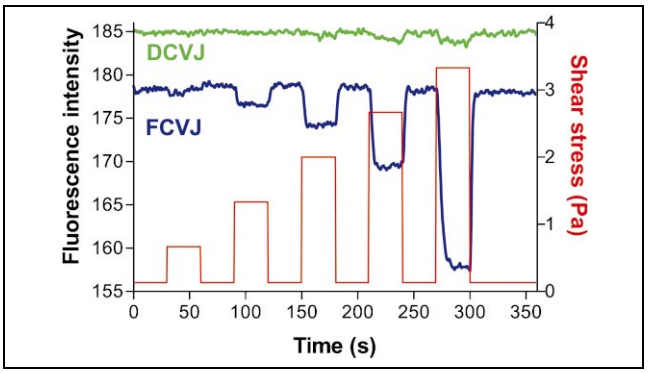

Fig. 5. Measured signal intensity of cells stained with DCVJ and FCVJ (**2g**) as a response to different step stimuli of shear stress. Both curves were subjected to a noise filter and an exponential correction for photobleaching. FCVJ shows a dramatically higher response. This allows a significantly higher sensitivity, while the noise component is greatly reduced.

2.3. *Measurement of membrane viscosity changes in cultured cells*

Step-shaped flow profiles of a successively rising magnitude were applied to the cell layer. In all cases, a marked decrease of emission intensity could be observed when flow was turned on, followed by a recovery of the intensity when the flow was turned off. To quantitatively analyze the sensitivity to shear stress, the average intensity of each phase of shear stress was subtracted from the average intensity during low shear stress (0.07 Pa), resulting in data pairs of intensity change over shear stress increase (Fig. 4). Linear regressions were computed from these data pairs, and tests for statistical significance (*t*-test) as well as the deviation from linearity (runs test) were performed. Compounds **2b**, **2c**, **2d** and FCVJ showed a higher amplitude of the intensity when used to probe shear stress in cells than DCVJ ($P < 0.0001$ for compounds **2b**, **2d** and FCVJ, $P = 0.07$ for **2c**). The data points (Fig. 4) showed no significant deviations from the straight line (runs test, values ranging from $P = 0.2$ for DCVJ to $P = 1.0$ for **2b**). These results, as well as the amplitude of the response, are summarized in Table 1.

FCVJ had the strongest response to shear stress. The amplitude of the fluorescence change in stained cells exposed to shear stress was more than 20 times higher than it could be observed with DCVJ. Fig. 5 shows the measured intensities of the fluorescence of DCVJ in comparison to FCVJ in stained cell membranes as a response to step changes of fluid shear stress of different magnitudes in an experimental set-up similar to the one described in [22]. The signal-to-noise ratio was significantly lower. While a statistically significant detection of shear stress with DCVJ was possible with values higher than 0.6 Pa [22], FCVJ allowed the detection of changes lower than 0.1 Pa (data not shown).

Microscope images indicated that rotors with longer chains exhibited slower migration rates and less intense cytoplasmic staining. In the confocal images (Fig. 6), nucleole staining became visible for compounds with shorter chains, including DCVJ and compound **2c**. Stained nucleoles were not visible for compounds **2d** and FCVJ. This indicates lower intracellular migration rates of these probes.

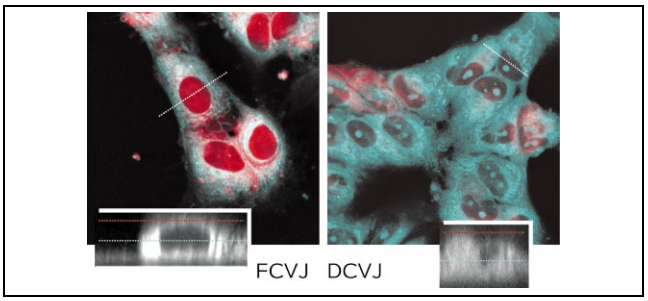

Fig. 6. False-color images of stained cells generated with a confocal microscope. Out of the *Z*-stack (small images), two planes have been selected: one plane through the middle of the cell (blue dashed line), colored blue, and one along the top of the cell (red dashed line), colored red. Both planes are overlaid, resulting in a red–blue image, where blue indicates cytoplasmic staining and red the staining in the cell membrane at the top of the cell. It can be seen that the membrane staining in the left image (FCVJ) is significantly higher than in the right image (DCVJ). Also, DCVJ exhibits nucleole staining, which cannot be observed with FCVJ. Cross sections in *Z*-direction along the white dotted lines in the upper image, which are displayed in the small lower images, also show a stronger fluorescence in the region above the nucleus for FCVJ, which cannot be seen with DCVJ.

The stability against photobleaching was also tested in compounds **2c**, **2g** and DCVJ. In a stained cell monolayer, all probes degraded under the influence of the excitation light in an exponential fashion. FCVJ (**2g**) showed a significantly higher stability against photobleaching than DCVJ. In a stained cell monolayer, all compounds degraded under the influence of the excitation light. With DCVJ, the half-life was 96 s. The half-life of compound **2c** was 70 s, and that of FCVJ was 112 s (Fig. 7), both significantly different from DCVJ ($P < 0.0005$).

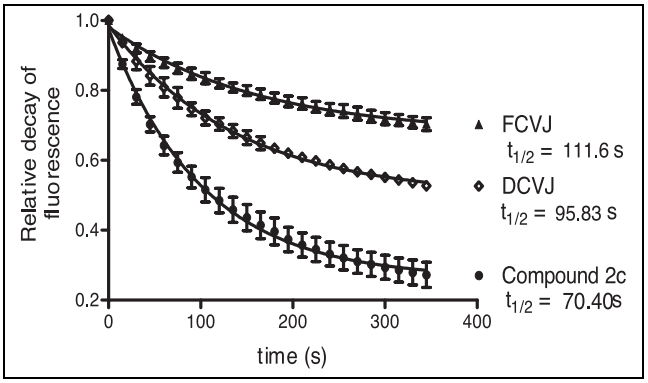

Fig. 7. Decay of fluorescence intensity of the probes in stained cells due to photobleaching. FCVJ shows a significantly higher decay half-time than DCVJ ($P < 0.0005$). Compound **2c**, however, is less stable than DCVJ.

3. Discussion

Most often, measurement of membrane viscosity is carried out using FRAP or fluorescence anisotropy. The method of FRAP is based on directing a focused laser beam at the cell membrane, which destroys the fluorescent dye in a defined region. Diffusion within the membrane allows dye from the neighboring environment to migrate into the bleached spot. The half-life of the fluorescence recovery is inversely proportional to the diffusion coefficient of the dye [23], which in turn is proportional to the fluidity. There are two major disadvantages associated with FRAP. Firstly, the measurement process is slow, since times between 20 and 60 s are required in order to allow sufficient recovery for the reliable determination of the half-life. This fact strongly limits the temporal resolution of any FRAP measurement and does not permit measurement of dynamic processes. Secondly, FRAP is limited in its resolution, as reduction of the radius of the bleached spot increases the error associated with the measurement. In addition, the bleaching pulse introduces power densities up to 1 MW/cm^2 to the membrane [23], leading both to the generation of free radicals by photolysis as well as local heating with potential damage to proteins [23]. Especially the second effect may cause artefacts, because the resulting cross-linking of the proteins [23] leads to decreased membrane diffusivity.

Membrane viscosity measurements by fluorescence anisotropy utilize the fact that certain molecules can only be excited by light waves in one polarization plane. The emitted light, again, is polarized. During the excited lifetime, the molecule can rotate, thus shifting the plane of emitted light. The ratio of emitted light parallel versus perpendicular to the plane of excitation is a nonlinear function of the viscosity [18]. While the spatial resolution is essentially determined by the limits of the microscope, rapid photobleaching of the probes both confines the maximum sensitivity and the exposure time of the probe to the excitation light. Furthermore, the polarizing filters in the emission light path generally absorb a significant portion of the emitted light. Moreover, it was shown in a recent study that the deformation of cells caused by shear stress may produce artifacts that are similar to an increase in membrane fluidity [24], which makes anisotropy observations difficult to interpret.

More recently, environment-sensitive probes have been used in membrane viscosity studies. In this category of fluorescent probes belong a group of compounds that have been shown to undergo intramolecular charge transfer when excited by photon absorption [25]. One member of the group, DCVJ (**1**), has been extensively characterized. For the intramolecular charge transfer, the julolidine group functions as the electron donor, and the dicyano-group as electron acceptor [25]. The relaxation of the excited state can either occur through photon emission or non-radiative processes [26]. When k_r and k_{nr} represent the rates of radiative and non-radiative relaxation, respectively, the quantum yield Φ is expressed by [26]:

$$\Phi = \frac{k_r}{k_r + k_{nr}} \tag{1}$$

Since the reorientation of the rotor, the process which leads to the non-radiative relaxation, is dependent on the free volume of the environment, the quantum yield depends on the temperature T and the viscosity η of the medium according to [26]:

$$\Phi \approx C'\left(\frac{\eta}{T}\right)^x \tag{2}$$

C' and x are constants. In a simplified form, and under the assumption of a constant temperature, this relationship is also known as the Förster–Hoffmann equation [27]:

$$\log\Phi = C + x\log\eta \tag{3}$$

For DCVJ, the constant x has been shown to be 0.6 [27]. Experiments that were conducted in media with different viscosities have confirmed Eq. 3 [1].

If the absorbed light intensity I_{ab} is known, the emission intensity I_{em} and the quantum yield are directly proportional through $I_{em} = I_{ab}\Phi$ [26]. Therefore, changes in the viscosity of the environment can be directly determined by measuring the emission intensities I_1 and I_2 before and after the viscosity change. With the corresponding viscosities η_1 and η_2, and under the assumption of constant temperature and constant absorption, Eq. 4 can be obtained [22]:

$$\frac{\eta_1}{\eta_2} = \left(\frac{\Phi_1}{\Phi_2}\right)\frac{1}{x} = \left(\frac{I_1 - I_0}{I_2 - I_0}\right)\frac{1}{x} \tag{4}$$

In Eq. 4, a background intensity I_0, the non-fluorescent amount of light caused by filter bleed-through, scatter and ambient light, has been allowed for. Depending on the measurement setup, the background intensity may not be negligible.

The assessment of membrane viscosity using molecular rotors overcomes the limits posed by FRAP or fluorescence anisotropy measurements. The spatial resolution of the method is potentially as high as it is for fluorescence anisotropy, because it is primarily limited by the optics of the microscope. The molecular rotor also responds to changes of viscosity almost instantaneously (within the nanosecond range) [25]. This allows a very high temporal resolution of the measurements, so that dynamic observations become possible.

The major disadvantage associated with DCVJ when used to probe cell membranes is the affinity for tubulin and proteins in the cytoplasm. The experiments presented in [15] are based on cultured cells, where a significant cytoplasmic staining exists, and a continuous exchange of the dye between the cytoplasm and the membrane takes

place. Both the cytoskeleton with its slow response to shear stress [28,29], and the cytoplasm, which slightly increases viscosity with shear stress [30], do not contribute to the signal measured, but provide a background fluorescence which reduces the measurement sensitivity. Furthermore, the relative intensity of the background is unknown and not easily determined, making quantitative measurements of membrane viscosity changes difficult.

To address the above issues encountered with DCVJ (and related rotors), we have synthesized several fluorescent probes, structurally related to DCVJ, with hydrophobic chains of different length attached to it. All probes synthesized showed a similar photophysical behavior to DCVJ with excitation and emission wavelengths in the same range. Also, the dependency of the quantum yield on the viscosity of the environment (slope x in Eq. 3) was similar. This shows that the modifications performed do not inhibit the function of the rotor, i.e. that the molecule can lose its excited state either through intramolecular rotation or through photon emission, depending on the viscosity of the environment.

Tests were performed to determine whether each compound is suitable for membrane viscosity measurements. In the first step, the fluorescent properties of each probe were determined. All compounds were similar in their physical properties. In the second step, solubility in aqueous media was determined, a prerequisite for the staining of attached cells. Both BSA and FCS may be used as a carrier. BSA binding was possible for all compounds except **2f**. The probes with shorter chains, **2a** through **2d**, as well as FCVJ, were also soluble in media prepared with FCS. Due to its carboxylic acid, **2a** is directly water-soluble. All compounds capable of binding to serum albumins were then tested for their cell staining capability. All compounds except **2a** and **2f** were able to stain cells. Finally, stained cells were submitted to shear stress, and the fluorescence intensity change as a function of the shear stress applied was recorded and compared between the compounds. Out of five probes tested (**2b** through **2e**, and **2g**), **2c** showed a similar response to DCVJ when used to test cells exposed to shear stress, while **2b**, **2d** and FCVJ showed a higher amplitude of the response.

FCVJ (**2g**), a rotor in which a farnesyl group was attached to the julolidine part via an ester bond, showed a superior response when probing cell membrane viscosity changes than all other probes, including DCVJ. Farnesyl is a hydrocarbon chain that improves membrane localization [31,32]. Substituting R for farnesyl (Fig. 1) resulted in a dye that shows an improved affinity for the cell membrane over DCVJ. This leads to a slower migration into the cytoplasm, a lower background signal and a higher signal-to-noise ratio in the measured intensity time-courses. The confocal images (Fig. 6) show that FCVJ can be found in the membrane at a higher concentration. With the given z-resolution of the confocal microscope, it is difficult to distinguish between the cell membrane on top of the nucleus and the cytoplasm layer between the nucleus and the membrane, but it is reasonable to assume that with an active exchange of the dye between the cytoplasm and the membrane, both layers would be stained.

According to the confocal images, DCVJ and the short-chained compound **2b** showed a high affinity for the cytoskeleton, and both dyes can be found in the nucleoles (Fig. 6). With compound **2d**, there is less tubulin staining and no nucleole staining. This suggests that longer chains allow a stronger binding of the dye to the membrane, and also reduces the migration into the inner compartments of the cell.

Experiments have shown that some of the compounds, particularly FCVJ, show a higher resistance to photobleaching, than DCVJ. This makes FCVJ a more adequate probe for long-term photophysical measurements. It should be noted that the half-life of DCVJ is about 50–100 times higher than the half-life of 1,6-diphenyl-2,3,5-hexatriene, a probe commonly used for viscosity measurements through fluorescence anisotropy under the same conditions.

The presented results show a significant improvement over DCVJ by combining a farnesyl chain with a molecular rotor with respect to membrane localization, stability against photobleaching, and sensitivity of membrane viscosity measurements. Membrane viscosity changes could be detected for fluid shear stress as low as 0.1 Pa, while DCVJ did not lead to statistically significant changes for shear stress values of 0.6 Pa and below [15]. However, cytoplasmic staining still persists even for FCVJ, which likely is a consequence of the cell metabolism. Further experiments are required to determine if the metabolic activity of the cell can be inhibited, and to what extent such an inhibition would affect the cell membrane viscosity.

4. Significance

Molecular rotors are new and promising tools for cell membrane viscosity measurements. One of the applications is the measurement of cell membrane viscosity in cultured cells or in vivo: membrane viscosity changes are crucial in the understanding of many signaling processes and diseases. Commercially available rotors such as DCVJ, however, are associated with disadvantages such as binding to the cell cytoskeleton and migration into inner compartments of the cell. While DCVJ allows the measurement of cell membrane viscosity changes, a higher sensitivity can be expected from DCVJ-derived molecules that show a higher affinity to the membrane.

We synthesized a group of related compounds that are composed of a DCVJ-like rotor and a hydrocarbon chain. These molecules retain their viscosity sensitivity, but show a higher affinity for the cell membrane with increasing chain length. This is generally associated with a higher

amplitude of the fluorescence intensity change that can be observed when changes of membrane viscosity occur. Notably the attachment of a farnesyl chain leads to a more than 20-fold increase in amplitude over DCVJ. This new molecular rotor, referred to as FCVJ, improved the signal-to-noise ratio, thereby allowing the measurement of far smaller viscosity changes than DCVJ.

5. Materials and methods

*5.1. Synthesis of aldehyde **4***

To a solution of julolidine (**3**) (0.5 g, 2.88 mmol) and *N*,*N*-dimethyl formamide (0.27 ml, 3.46 mmol) in dichloromethane (5 ml), was added dropwise phosphorous oxychloride (0.29 ml, 3.17 mmol) and the mixture was stirred at 25°C for 8 h. The reaction was treated with an aqueous solution of sodium hydroxide (2 M) and the mixture was stirred at 0°C for 4 h. The organic layer was extracted with ethyl ether (3×10 ml), collected, dried ($MgSO_4$) and concentrated under reduced pressure. The residue was crystallized twice from dichloromethane/hexane (1:10) to afford aldehyde **4** (0.55 g, 2.74 mmol, 95% yield). **4**: Colorless solid; $R_f = 0.37$ (silica, 30% ethyl ether in hexanes); ^{1}H NMR (400 MHz, $CDCl_3$) δ 9.58 (s, 1 H), 7.28 (s, 2H), 3.27–3.29 (m, 4H), 2.74–2.76 (m, 4H), 1.94–1.96 (m, 4H); ^{13}C NMR (100 MHz, $CDCl_3$) δ 189.9, 147.7, 129.3, 123.8, 120.2, 50.0, 27.7, 21.3; HRMS, calcd for $C_{13}H_{15}NO$ ($M+H^+$) 202.2754, found 202.2761.

*5.2. Synthesis of farnesyl ester **7g***

To a solution of cyanoacetic acid (**5**) (0.43 g, 5 mmol) and *trans*,*trans*-farnesol (**6g**) (1.11 g, 5 mmol) in dichloromethane (5 ml) was added DCC (1.03 g, 5 mmol) and the mixture was stirred at 25°C for 10 h. The reaction was then diluted with dichloromethane (20 ml) and the formed DCU was filtered under gravity. The filtrate was dried ($MgSO_4$) and concentrated and the residue was purified by column chromatography (silica, 5–10% ethyl ether in hexane) to afford farnesyl ester **7g** (1.39 g, 4.8 mmol, 96% yield). **7g**: Colorless oil; $R_f = 0.63$ (silica, 30% ethyl ether in hexanes); IR (film) ν_{max} 2968.6, 2931.2, 2857.7, 1757.9, 1669.5, 1448.7, 1383.2, 1349.0, 1327.3, 1274.7, 1181.9, 985.5, 932.7; ^{1}H NMR (400 MHz, $CDCl_3$) δ 5.33 (t, 1H), 5.05–5.08 (m, 2H), 4.68–4.71 (d, 2H), 3.44 (s, 2H), 1.9–2.18 (m, 8H), 1.71 (s, 3H), 1.66 (s, 3H), 1.58 (s, 6H); ^{13}C NMR (100 MHz, $CDCl_3$) δ 162.7, 143.9, 135.3, 131.0, 124.0, 123.1, 116.7, 112.9, 63.5, 39.6, 39.4, 26.7, 26.1, 25.7, 24.7, 17.7, 16.5, 16.0; HRMS, calcd for $C_{18}H_{27}NO_2$ ($M+H^+$) 290.2120, found 290.2141.

*5.3. Synthesis of FCVJ **2g***

To a solution of farnesyl cyanoacetic ester (**7g**) (1.08 g, 3.73 mmol) and aldehyde **4** (0.5 g, 2.48 mmol) in tetrahydrofuran (15 ml) was added triethylamine (0.7 ml, 5 mmol) and the mixture was stirred at 50°C for 10 h. After consumption of the starting material, the reaction mixture was concentrated and the residue purified by column chromatography (silica, 10% ethyl ether in hexane) to afford FCVJ (**2g**) (1.1 g, 2.36 mmol, 95% yield). Compound **2g** was crystallized twice from ether/hexane. FCVJ: Yellow orange solid; $R_f = 0.34$ (silica, 30% ethyl ether in hexanes); IR (film) ν_{max} 2931.4, 2210.6, 1708.0, 1613.4, 1571.6, 1522.3, 1442.9, 1316.5, 1227.1, 1163.1, 1095.8; ^{1}H NMR (400 MHz, $CDCl_3$) δ 7.93 (s, 1H), 7.50 (s, 2H), 5.42–5.43 (t, 1H), 5.08–5.10 (m, 2H), 4.76–4.78 (d, 2H), 3.30–3.33 (m, 4H), 2.72- 2.76 (m, 4H), 1.90–2.20 (m, 8H), 1.74 (s, 3H), 1.67 (s, 3H), 1.60 (s, 6H); ^{13}C NMR (100 MHz, $CDCl_3$) δ 164.6, 154.1, 147.3, 142.1, 135.2, 131.4, 131.1, 124.2, 123.5, 120.6, 118.3, 118.1, 117.9, 91.7, 62.6, 50.2, 39.7, 39.6, 27.6, 26.8, 26.3, 25.8, 21.2, 17.8, 16.7, 16.1; HRMS, calcd for $C_{31}H_{40}N_2O_2$ ($M+H^+$) 473.3168, found 473.3189.

Probe **2b**: Red solid; $R_f = 0.30$ (silica, 40% ethyl ether in hexanes); IR (film) ν_{max} 2947.9, 2209.6, 1711.8, 1613.1, 1569.6, 1521.0, 1435.3, 1317.2, 1295.8, 1231.2, 1163.0, 1097.5; ^{1}H NMR (400 MHz, $CDCl_3$) δ 7.94 (s, 1H), 7.50 (s, 2H), 3.86 (s, 3H), 3.31–3.34 (m, 4H), 2.72–2.74 (m, 4H), 1.94–1.96 (m, 4H); ^{13}C NMR (100 MHz, $CDCl_3$) δ 165.1, 154.3, 147.5, 131.6, 120.7, 118.2, 118.1, 90.9, 52.7, 50.2, 27.6, 21.2; HRMS, calcd for $C_{17}H_{18}N_2O_2$ ($M+H^+$) 283.1446, found 283.1461.

Probe **2c**: Red solid; $R_f = 0.36$ (silica, 40% ethyl ether in hexanes); IR (film) ν_{max} 2937.1, 2209.7, 1708.8, 1613.2, 1570.4, 1522.3, 1443.2, 1317.7, 1294.6, 1231.5, 1164.2, 1097.5, 1021.3; ^{1}H NMR (400 MHz, $CDCl_3$) δ 7.91 (s, 1 H), 7.48 (s, 2H), 4.28–4.31 (m, 2H), 3.29–3.32 (m, 4H), 2.71–2.74 (m, 4H), 1.93–1.95 (m, 4H), 1.33–1.37 (m, 3H); ^{13}C NMR (100 MHz, $CDCl_3$) δ 164.5, 154.0, 147.4, 131.4, 120.6, 118.2, 117.9, 91.4, 61.6, 50.1, 27.6, 21.1, 14.4; HRMS, calcd for $C_{18}H_{20}N_2O_2$ ($M+H^+$) 297.1603, found 297.1611.

Probe **2d**: Orange red solid; $R_f = 0.39$ (silica, 40% ethyl ether in hexanes); IR (film) ν_{max} 2956.0, 2209.3, 1707.9, 1613.0, 1569.9, 1521.3, 1442.9, 1316.9, 1228.4, 1163.5, 1097.8; ^{1}H NMR (400 MHz, $CDCl_3$) δ 7.93 (s, 1 H), 7.50 (s, 2H), 4.23–4.27 (m, 2H), 3.30–3.33 (m, 4H), 2.72–2.76 (m, 4H), 1.94–1.97 (m, 4H), 1.43–1.72 (m, 4H), 0.94–0.98 (m, 3H); ^{13}C NMR (100 MHz, $CDCl_3$) δ 184.7, 164.7, 154.1, 131.5, 120.6, 118.3, 65.5, 50.2, 30.8, 27.7, 21.2, 19.2, 13.9; HRMS, calcd for $C_{20}H_{24}N_2O_2$ ($M+H^+$) 325.4246, found 325.4250.

Probe **2e**: Orange yellow solid; $R_f = 0.40$ (silica, 40% ethyl ether/hexanes); IR (film) ν_{max} 2925.9, 2853.1, 2210.5, 1709.5, 1613.0, 1571.6, 1522.6, 1443.3, 1317.2, 1229.4, 1163.0, 1099.9; ^{1}H NMR (400 MHz, $CDCl_3$) δ 7.93 (s, 1 H), 7.50 (s, 2H), 4.22–4.24 (m, 2H), 3.30–3.33 (m, 4H), 2.72–2.76 (m, 4H), 1.94–1.97 (m, 4H), 1.68–1.75 (m, 2H), 1.25–1.45 (m, 16H), 0.86–0.89 (m, 3H); ^{13}C NMR (100 MHz, $CDCl_3$) δ 164.6, 154.1, 147.4, 131.5, 120.6, 118.3, 117.9, 91.7, 65.8, 50.2, 31.9, 29.6, 29.4, 29.3, 28.7, 27.6, 25.9, 22.8, 21.2, 14.3 HRMS, calcd for $C_{26}H_{36}N_2O_2$ ($M+H^+$) 409.2855, found 409.2861.

Probe **2f**: Orange yellow solid; $R_f = 0.45$ (silica, 40% ethyl ether in hexanes); IR (film) ν_{max} 2917.4, 2849.9, 1715.5, 1570.7, 1521.1, 1444.3, 1316.3, 1234.4, 1165.3, 1101.5; ^{1}H NMR (400 MHz, $CDCl_3$) δ 7.93 (s, 1 H), 7.50 (s, 2H), 4.22–4.24 (m, 2H), 3.30–3.33 (m, 4H), 2.72–2.76 (m, 4H), 1.94–1.97 (m, 4H), 1.43–1.72 (m, 6H), 1.24–1.26 (m, 30H), 0.85–0.89 (m, 3H); ^{13}C NMR

(100 MHz, $CDCl_3$) δ 164.7, 154.1, 147.4, 131.5, 131.4, 120.6, 118.3, 117.9, 65.8, 50.2, 32.0, 29.8, 29.7, 29.6, 29.5, 29.4, 28.8, 27.7, 25.9, 22.8, 21.2, 14.3 HRMS, calcd for $C_{36}H_{56}N_2O_2$ ($M+H^+$) 549.4420, found 549.4439.

For the determination of the relationship between quantum yield and viscosity of the medium, mixtures of ethylene glycol and glycerol were prepared. Different viscosities were achieved through different vol/vol mixture ratios of ethylene glycol:glycerol as follows: 7:3 (49 cP), 5:5 (115 cP), 4:6 (163 cP), 3:7 (245 cP), 2:8 (391 cP) following an experiment described in [33]. 3.5 ml of each of these mixtures was filled into a spectroscopic cuvette under addition of 10 μl of probe stock solution (10 mM probe in methanol). The emission intensity of each of the five samples was acquired using an RF-1501 fluorophotospectrometer (Shimadzu, Kyoto, Japan) set at $\lambda_{excitation} = 455$ nm and $\lambda_{emission} = 505$ nm.

For the experiments on cultured cells, procedures similar to the ones described elsewhere [15] were used. Briefly, human umbilical cord endothelial cells were harvested using fresh umbilical cords, where the veins were treated with a 0.02% solution of collagenase in phosphate-buffered saline solution for 30 min at 25°C [34]. The cells were suspended in culture medium (Medium M199 with 2 mM L-glutamine, 50 U/ml penicillin, 50 μg/ml streptomycin and 20% FCS) and seeded on tissue culture dishes. These dishes were kept in the incubator at 37°C in CO_2 enriched air (5% CO_2) until confluency was reached. Once confluency was achieved, the cells were lifted with cell dissociation solution and resuspended in Dulbecco's modified Eagle's medium with 20% FCS at a concentration of 2.5×10^6 cells/ml. Aliquots of 350 μl of the suspension were used to seed the cells on glass slides (dimensions 10×40 mm) that were previously treated for 2 h with 0.5 M NaOH. The cells attached and formed a confluent layer within 24 h.

A staining solution was prepared from 50 μl stock solution of 20 mM of the examined probe in dimethyl sulfoxide (DMSO), which was dispersed in 2 ml FCS under vigorous stirring. 10 ml medium M199 was added. The slides with the cells were covered with the staining solution. Incubation took place over 10 min in the dark at 37°C. After the incubation period, the cells were rinsed with HBSS, and the fluorescence checked under an epifluorescent microscope (Diaphot TMD, Nikon, Garden City, NY, USA) using the G2B filter set. Flow chambers were assembled using a standard methacrylate spectroscopic cuvette (Fisher Scientific, Pittsburgh, PA, USA) and a parallel-plate black Delrin flow chamber with a channel width of 6 mm and a depth of 500 μm. The flow channel was formed between the flow chamber wall and the glass slide with the confluent cell monolayer. In the parallel-plate flow chamber, the following relationship between flow Q and wall shear stress τ holds:

$$\tau = \frac{6\mu Q}{h^2 w} \tag{5}$$

where μ is the viscosity of the medium, h is the channel depth and w is the channel width. On the Shimadzu RF-1501 fluorophotospectrometer with time-course module, excitation wavelength was set to 455 nm, and emission wavelength to 505 nm. An additional 475 nm LP emission filter (Chroma, Brattleboro, VT, USA) blocked scattered blue light. A microcontroller-driven syringe pump (Pump 22, Harvard Apparatus, Holliston, MS, USA) attached to a PC provided a controlled flow of the flow medium, HBSS. Throughout the experiments, a minimum flow of 1 ml/min was maintained in order to provide the cells with fresh medium and avoid hypoxia. This minimal flow caused a shear stress of 0.07 Pa. Shear stress rates of 0.67, 1.33, 2.0, 2.67 and 3.33 Pa (1 Pa = 10 dyn/cm^2) were applied successively for 30 s with a 30 s period of 0.07 Pa in between. The drop in fluorescence intensity was determined for each step change of shear stress and plotted over the shear stress value. To determine the amplitude of the response, a straight line fit was performed (least-squares method) with the slope of this line representing the amplitude and the deviation from linearity determined with the runs test.

Summarized, the following tests were performed for each compound (not all of the tests have been performed on all of the compounds):

1. Basic properties: acquisition of excitation and emission spectra of the probe dissolved in DMSO at a concentration of 60 μM.
2. Solubility in water, FCS and BSA, as well as cell culture media with 20% FCS and 3% BSA, respectively.
3. Dependency of the quantum yield on the viscosity of the solvent.
4. Capability of the dye to stain cells.
5. Response of the quantum yield of the compound in cells to fluid shear stress.

For DCVJ and compounds **2b**, **2c**, **2g**, confocal images were acquired to more accurately determine the localization of the dye. *Z*-Sections of 200 μm thickness were obtained on a BioRad MRC-1024 confocal microscope using the FITC program. For DCVJ as well as compounds **2c** and **2g**, the resistance against photobleaching was tested by acquiring one image of the stained cells every 15 s using the epifluorescent microscope. In each of three independent experiments, the average intensity of the confluent cell area in the field of view was determined in each frame using Scion Image (Scion, Frederick, NY, USA). A one-phase exponential decay curve was fitted into the data points and the half-life of the compound was calculated.

Acknowledgements

This research was partially supported by the National Heart, Lung and Blood Institute Grant HL-40696 and by the American Cancer Society (RPG CDD-9922901). M.A.H. is the recipient of the National Research Service Award Fellowship from the National Institute of Health 1F32GM20476-01.

References

[1] C.E. Kung, J.K. Reed, Microviscosity measurements of phospholipid

bilayers using fluorescent dyes that undergo torsional relaxation, Biochemistry 25 (1986) 6114–6121.
[2] W.R. Dunham, R.H. Sands, S.B. Klein, E.A. Duelli, L.M. Rhodes, C.L. Marcelo, EPR measurements showing that plasma membrane viscosity can vary from 30 to 100 cP in human epidermal cell strains, Spectrochim. Acta A 52 (1996) 1357–1368.
[3] J. Kapitulnik, E. Weil, R. Rabinowitz, M.M. Krausz, Fetal and adult human liver differ markedly in the fluidity and lipid composition of their microsomal membranes, Hepatology 7 (1987) 55–60.
[4] M. Shinitzky, Membrane fluidity and cellular functions, in: M. Shinitzky (Ed.), Physiology of Membrane Fluidity, CRC Press, Boca Raton, FL, 1984, pp. 1–51.
[5] D.H. Rohrbach, R. Timpl, Molecular and Cellular Aspects of Basement Membranes, Academic Press, San Diego, CA, 1993.
[6] G. Deliconstantinos, V. Villiotou, J.C. Stavrides, Modulation of particulate nitric oxide synthase activity and peroxynitrite synthesis in cholesterol enriched endothelial cell membranes, Biochem. Pharmacol. 49 (1995) 1589–1600.
[7] M. Shinitzky, Membrane fluidity in malignancy. Adversative and recuperative, Biochim. Biophys. Acta 738 (1984) 251–261.
[8] M.M. Gleason, M.S. Medow, T.N. Tulenko, Excess membrane cholesterol alters calcium movements, cytosolic calcium levels, and membrane fluidity in arterial smooth muscle cells, Circ. Res. 69 (1991) 216–227.
[9] O. Nadiv, Y. Zick et al., Elevated protein tyrosine phosphatase activity and increased membrane viscosity are associated with impaired activation of the insulin receptor kinase in old rats, Biochem. J. 298 (1994) 443–450.
[10] W. Osterode, C. Holler, F. Ulberth, Nutritional antioxidants, red cell membrane fluidity and blood viscosity in type 1 (insulin-dependent) diabetes mellitus, Diabet. Med. 13 (1996) 1044–1050.
[11] K. Scheuer, A. Maras, W.F. Gattaz, N. Cairns, H. Forstl, W.E. Muller, Cortical NMDA receptor properties and membrane fluidity are altered in Alzheimer's disease, Dementia 7 (1996) 210–214.
[12] R.B. Scott, J.M. Collins, P.A. Hunt, Alzheimer's disease and Down syndrome: leukocyte membrane fluidity alterations, Mech. Ageing Dev. 75 (1994) 1–10.
[13] C. Maczek, G. Bock, G. Jurgens, D. Schonitzer, H. Dietrich, G. Wick, Environmental influence on age-related changes of human lymphocyte membrane viscosity using severe combined immunodeficiency mice as an in vivo model, Exp. Gerontol. 33 (1998) 485–498.
[14] K. Shiraishi, S. Matsuzaki, H. Ishida, H. Nakazawa, Impaired erythrocyte deformability and membrane fluidity in alcoholic liver disease: participation in disturbed hepatic microcirculation, Alcohol Alcoholism 28 (Suppl. 1A) (1993) 59–64.
[15] M.A. Haidekker, N. L'Heureux, J.A. Frangos, Fluid shear stress increases membrane fluidity in endothelial cells: a study with DCVJ fluorescence, Am. J. Physiol Heart Circ. Physiol. 278 (2000) H1401–H1406.
[16] P.F. Davies, Flow-mediated endothelial mechanotransduction, Physiol. Rev. 75 (1995) 519–560.
[17] D. Axelrod, D.E. Koppel, J. Schlessinger, E. Elson, W.W. Webb, Mobility measurement by analysis of fluorescence photobleaching recovery kinetics, Biophys. J. 16 (1976) 1055–1069.
[18] M. Shinitzky, Y. Barenholz, Fluidity parameters of lipid regions determined by fluorescence polarization, Biochim. Biophys. Acta 515 (1978) 367–394.
[19] T. Parasassi, M. Di Stefano, M. Loiero, G. Ravagnan, E. Gratton, Cholesterol modifies water concentration and dynamics in phospholipid bilayers: a fluorescence study using Laurdan probe, Biophys. J. 66 (1994) 763–768.
[20] R.O. Loutfy, Fluorescence probes for polymer free-volume, Pure Appl. Chem. 58 (1986) 1239–1248.
[21] C.E. Kung, J.K. Reed, Fluorescent molecular rotors: a new class of probes for tubulin structure and assembly, Biochemistry 28 (1989) 6678–6686.
[22] M.A. Haidekker, J.A. Frangos, A fluorescent molecular rotor for the study of membrane fluidity in endothelial cells under fluid shear stress, in: D.L. Farkas, R.C. Leif (Eds.), Optical Diagnostics of Living Cells III, Proceedings of SPIE, 2000, pp. 101–112.
[23] M. Edidin, Fluorescence photobleaching and recovery, FPR, in the analysis of membrane structure and dynamics, in: S. Damjanovich et al. (Eds.), Mobility and Proximity in Biological Membranes, CRC Press, Boca Raton, FL, 1994, pp. 109–135.
[24] H. Abdul-Rahim, M. Bouchy, Analysis of the fluorescence anisotropy of labelled membranes submitted to a shear stress, J. Photochem. Photobiol. B: Biol. 47 (1998) 95–108.
[25] J.E. Kuder, W.W. Limburg, J.M. Pochan, D. Wychick, Structural effects on the electrochemistry and charge distribution of mono-, di-, and tri-cyanovinyl aromatic compounds, J. Chem. Soc. Perkins Trans. 2 (1977) 1643–1651.
[26] M.L. Viriot, M.C. Carré, C. Geoffroy-Chapotot, A. Brembilla, S. Muller, J.-F. Stoltz, Molecular rotors as fluorescent probes for biological studies, Clin. Hemorheol. Microcirc. 19 (1998) 151–160.
[27] Th. Förster, G. Hoffmann, Die Viskositätsabhängigkeit der Fluoreszenzquantenausbeuten einiger Farbstoffsysteme (Effect of viscosity on the fluorescence quantum yield of some dye systems), Z. Phys. Chem. 75 (1971) 63–76.
[28] C.G. Galbraith, R. Skalak, S. Chien, Shear stress induces spatial reorganization of the endothelial cell cytoskeleton, Cell Motil. Cytoskeleton 40 (1998) 317–330.
[29] A. Cucina, D.L. Santoro et al., Shear stress induces changes in the morphology and cytoskeleton organisation of arterial endothelial cells, Eur. J. Vasc. Endovasc. Surg. 9 (1995) 86–92.
[30] W. Möller, S. Takenaka, M. Rust, W. Stahlhofen, J. Heyer, Probing mechanical properties of living cells by magnetopneumography, J. Aerosol. Med. 10 (1997) 171–186.
[31] V.D. Barbu, Isoprenylation of proteins: what is its role?, C.R. Seances Soc. Biol. Fil. 185 (1991) 278–289.
[32] N.E. Kohl, M.W. Conner, J.B. Gibbs, S.L. Graham, G.D. Hartman, A. Oliff, Development of inhibitors of protein farnesylation as potential chemotherapeutic agents, J. Cell Biochem. 22 (Suppl.) (1995) 145–150.
[33] T. Iwaki, C. Torigoe, M. Noji, M. Nakanishi, Antibodies for fluorescent molecular rotors, Biochemistry 32 (1993) 7589–7592.
[34] F. Berthiaume, J.A. Frangos, Fluid flow increases membrane permeability to merocyanine 540 in human endothelial cells, Biochim. Biophys. Acta 1191 (1994) 209–218.